Macromolecules

ARTICLE

pubs.acs.org/Macromolecules

Distribution of Glass Transition Temperatures in Free-Standing, Nanoconfined Polystyrene Films: A Test of de Gennes' Sliding Motion Mechanism

Soyoung Kim[†] and John M. Torkelson[*,†,‡]

[†]Department of Chemical and Biological Engineering and [‡]Department of Materials Science and Engineering, Northwestern University, Evanston, Illinois 60208, United States

Supporting Information

ABSTRACT: Effects of nanoscale confinement on the distribution of glass transition temperatures (T_gs) in free-standing polystyrene (PS) films are determined via a multilayer/self-referencing fluorescence method employing a pyrene dye label. Average film T_gs yield a T_g-confinement effect in agreement with the molecular weight (MW) dependence reported by Forrest, Dalnoki-Veress, and Dutcher. Multilayer films, with one pyrene-labeled layer, reveal that a 14 nm thick free-surface layer in sufficiently thick films ($\geq\sim$56 nm) exhibits $T_g = T_{g,bulk} - \sim$34 K, independent of film thickness and indicative of a strong T_g gradient near a surface. In sufficiently thin films ($\leq\sim$56 nm), a 14 nm thick free-surface layer reports T_g that decreases with decreasing film thickness and is equal to the T_g of a 14 nm thick middle layer and the average film T_g. Thus, the strongly perturbed T_g at the two surfaces affects T_g several tens of nanometers into and across the film, resulting in greater T_g reductions than observed in supported films. This study also tests de Gennes' "sliding motion mechanism", devised to explain the MW dependence of the T_g-confinement effect in free-standing films. No midlayer chain in a multilayer film forms loops or bridges reaching a surface. de Gennes' mechanism indicates that T_g reductions occur only at locations where segments are present from chains forming loops or bridges at a surface. Major T_g reductions (as large as $\sim$54 K below $T_{g,bulk}$) are observed in midlayers of nanoconfined free-standing PS films, disproving a key premise of the mechanism.

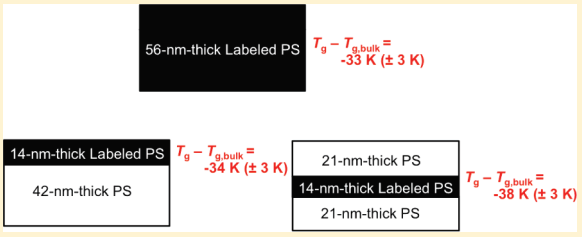

INTRODUCTION

In 1994, Keddie, Jones, and Cory[1,2] published the first systematic studies of the effect of confinement on the glass transition temperature (T_g) of thin polymer films. Using ellipsometry to characterize T_g via measurement of thickness as a function of temperature, they observed reductions in T_g with decreasing thickness in ultrathin polystyrene (PS) films supported on silica and ultrathin poly(methyl methacrylate) (PMMA) films supported on gold. They observed no significant molecular weight (MW) dependence of the T_g-confinement effect and hypothesized that the reduction in T_g with nanoscale confinement resulted from a liquidlike layer at the free surface with increased mobility relative to bulk polymer.[1]

Since then, many experimental and theoretical studies have focused on characterizing and understanding the effect of nanoconfinement on T_g and assorted, related behavior of polymers in thin film geometries.[3−7] Numerous experimental studies have investigated average T_gs of thin polymer films. The film geometry provides the combined advantages of ease in quantitatively tuning the level of confinement via spin-coating[8] and simple application with a range of methods for determining T_g. Most often, these studies have concentrated on single-layer PS films supported on silica substrates. There is general agreement among these studies that T_g decreases with decreasing thickness for nanoconfined, supported PS films with one free surface.[3−7,9]

By using fluorophores to label a single layer within a multilayer PS film, Ellison and Torkelson[10] performed the first direct measurement of T_g gradients in substrate-supported PS films. They measured T_g at specific, targeted film locations, showing that the T_g of a 14 nm thick PS free-surface layer atop a bulk PS layer is reduced $\sim$32 K from its bulk value, consistent with the idea that the T_g-confinement effect in PS films originates from a reduction in the free-surface layer T_g. With the multilayer/fluorescence method, they also showed that the perturbation to T_g in the free-surface layer can propagate into a substrate-supported PS film and perturb the glass transition response several tens of nanometers away from the free surface. They further demonstrated that the extent to which the local T_g smoothly transitions from a reduced value near the free surface to bulk behavior in the film interior depends strongly on nanoconfinement.[10] Multilayer/fluorescence studies have revealed related behavior in other systems,[11−16] including ones in which there are hydrogen-bonding interactions at polymer−substrate interfaces leading to an increase in polymer T_g. These methods have recently been adapted for related investigations

Received: March 17, 2011
Revised: April 29, 2011
Published: May 10, 2011

involving neutron reflectivity measurements[17] on multilayer films of hydrogenated and deuterated PS and dielectric spectroscopy studies of multilayer films with one layer containing polymer labeled at low levels with a high dipole moment dye.[18]

In a related molecular dynamics simulation study, Peter et al.[19] found that average cooperative dynamics in a film are accelerated due to a smooth gradient in relaxation originating from the free surface, where segmental relaxation occurs much faster than in the bulk. Further experimental support for enhanced mobility at the surface of polymer films comes from a variety of sources. For example, Fakhraai and Forrest[20] produced well-defined nanodeformations on the surface of supported PS films. They observed surface relaxation over a 277−369 K temperature range, far below $T_{g,bulk}$ and consistent with enhanced free-surface mobility. Tsui and co-workers[21] studied the viscosity of unentangled, short-chain supported PS films, obtaining a Kauzmann temperature, T_K, as a function of thickness by application of a Vogel−Fulcher−Tamman equation to the experimentally determined temperature-dependent viscosity. They found a reduction in T_K with decreasing thickness below 20 nm. From hydrodynamic analysis and application of a two-layer model, they interpreted that a highly mobile surface liquid layer was present with a thickness of less than 2.3 nm and indicated that this mobile surface layer is responsible for the effects of confinement on the effective viscosity and the T_g of PS films.

In contrast to the many dozens of investigations of the T_g-confinement effect and related behavior of polymer films supported on silica, fewer studies have focused on the T_g-confinement effect and related properties of single-layer free-standing films,[22−47] i.e., films with two polymer−air interfaces or free surfaces. Using Brillouin scattering and ellipsometry, Dutcher and co-workers[22−27] were the first group to characterize the T_g-confinement effect in free-standing polymer films, doing studies on PS and PMMA. The most striking features associated with their free-standing PS film studies are that the T_g reductions can be much greater than those of PS films supported on silica (T_g reductions as large as 70−80 K were reported in free-standing films relative to bulk T_g[22−25]) and that at high MW there is a strong MW dependence of the T_g reduction.

Unlike free-standing PS films, in supported PS films there is no significant MW dependence of the T_g-confinement effect.[48] This difference between free-standing and supported PS films is one of the most intriguing results to arise from studies of the effects of nanoscale confinement on glass-formers. de Gennes[29] proposed a simple physical picture of "sliding motion" to explain the chain-length dependence of T_g in nanoconfined, free-standing films. He suggested that the mobility of a polymer chain can be greatly enhanced if loops or bridges from the chain extend to the surface region of the thin film. In de Gennes' mechanism, the loops of a chain present at a free surface can transport "kinks" of free volume along the chain's own length, allowing for faster structural relaxation and thereby inducing a reduction in local T_g. The model leads to a function $T_g(z)$ which depends on the distance z from a free surface. As a result of the sliding motion, T_g is expected to decrease in regions near the free surface at distances comparable to the size of a polymer coil (i.e., the diameter of the volume pervaded by a chain) because additional free volume can presumably be transported from the loops at the free surface over a thickness related to coil diameter. Conversely, with de Gennes' mechanism, bulk T_g is expected in interior regions of the film where no polymer chain is present that has segments forming loops at the free surface. This mechanism provides a potential explanation for the important role of MW on the T_g-confinement effect in PS free-standing films and suggests a (semi)quantitative approach, based on the MW dependence of the polymer coil radius, to explain this behavior.

Here we employ a recently developed multilayer/self-referencing fluorescence method that yields T_g values within surface and interior layers of known thickness. First reported in 2008, the self-referencing fluorescence method was developed to measure the T_g-confinement effect in single-layer free-standing PS films via the temperature dependence of a fluorescence intensity ratio associated with a pyrenyl dye labeled to the polymer.[47] In most previous fluorescence studies of T_g-confinement effects, fluorescence intensity (at a specific wavelength or integrated over the whole spectrum) was measured as a function of temperature, with T_g being obtained from the intersection of the temperature dependences of the rubbery-state and glassy-state fluorescence intensities.[6,10−16,48,49] However, such measurements do not yield accurate and precise T_g determinations in free-standing films due to film rippling upon cooling, resulting in changes in the surface area of the film exposed to fluorescence excitation light. Many pyrene-based dyes can exhibit strong sensitivity of fluorescence spectral shape to nanoscale environment,[50−54] and we discovered that the spectral shape of a pyrene dye covalently attached in a particular way to PS changes as a function of temperature.[47] In turn, the use of an intensity ratio to characterize the changes in spectral shape provides an accurate and precise self-referencing determination of T_g, independent of any change in the surface area of the film exposed to fluorescence excitation caused by film rippling.[47] In our 2008 study, data obtained by self-referencing fluorescence for average T_gs across single-layer free-standing PS films[47] were in reasonable agreement with results of Dutcher and co-workers;[22−25] a major reduction in T_g was evident with decreasing thickness in films thinner than 80−90 nm, and the limited data set agreed with the MW dependence of the T_g-confinement effect reported by Dutcher and co-workers.

In particular, we have designed our current multilayer/fluorescence study to provide the first critical experimental test of de Gennes' sliding motion model in free-standing PS films.[29] By preparing trilayer films in which the middle layer contains pyrene-labeled PS and the two surface layers contain neat PS without pyrene dye, we demonstrate for the first time that a major reduction in T_g can be observed in the middle layer of nanoconfined free-standing polymer films even when the chains within that layer are unable to form loops at either of the two free surfaces. This contradicts a key premise of de Gennes' model. We further compare our results for the distribution of T_gs within free-standing nanoconfined PS films to those reported by Ellison and Torkelson[10] for supported nanoconfined PS films, demonstrating substantial agreement between the distributions of local T_g in these systems.

EXPERIMENTAL SECTION

1-Pyrenylmethyl methacrylate-labeled PS (MApyrene-labeled PS;[47] M_n = 805 000 g mol^{-1}, M_w/M_n = 1.31, by gel permeation chromatography (GPC) relative to PS standards using tetrahydrofuran (THF) as eluent) was synthesized by bulk free radical polymerization of styrene (Aldrich) in the presence of trace amounts of 1-pyrenylmethyl methacrylate (MApyrene; Polysciences). The MApyrene-labeled PS was precipitated into excess methanol and washed by redissolving in THF and precipitating in methanol seven times to remove any residual

dye-labeled monomer before drying under vacuum. (The unusually low PDI for the MApyrene-labeled PS resulted from the method employed during the multiple dissolution/precipitation steps used in removing unreacted dye-labeled monomer. With relatively weak precipitation conditions, there was a loss of lower MW fractions of the polymer, thereby resulting in a PDI that was well below 1.5 even though the polymer was synthesized by conventional free radical polymerization.) Bulk T_g values were measured by differential scanning calorimetry (DSC) (Mettler-Toledo 822e, second heat, onset method, 10 K/min) and fluorescence methods (temperature dependence of intensity ratios) agreed within experimental error: $T_{g,bulk}$ = 373 K by DSC and fluorescence. The pyrene label content was 1.2 mol % relative to all polymer repeat units as measured by UV−vis absorbance (Perkin-Elmer Lambda 35).

Polystyrene, with a reported M_n = 849 000 g mol^{-1} and M_w/M_n = 1.06, was used as received from Pressure Chemical. The onset bulk T_g value was measured as 373 K by a DSC Mettler-Toledo 822e (second heat, onset method, 10 K/min).

Single-layer free-standing films were fabricated by using a water transfer technique.[55] Related details are discussed in ref 47. Film thickness was verified by spin-coating a second film at the same time from the same solution onto a silicon slide with its native silicon oxide layer and measuring its thickness via spectroscopic ellipsometry (J.A. Woollam Co. M-2000D).

Bilayer and trilayer free-standing films were also fabricated by the water transfer technique.[55] Each layer was first prepared by spin-coating[8] dilute PS solutions onto freshly cleaved mica. These mica-supported individual layers were annealed separately at $T_{g,bulk}$ + 20 K for 12 h under vacuum to remove residual solvent prior to floating. The thickness of each layer was verified by spin-coating a second film at the same time from the same solution onto a silicon slide with a native silicon oxide layer and measuring its thickness via ellipsometry (J.A. Woollam Co. M-2000D). Multilayer films were assembled by sequentially floating them onto underlying polymer layers supported by mica. Excess water was evaporated under ambient conditions for at least 12 h before the next layer was added. Once assembled, all films were placed in a vacuum oven at room temperature for at least 12 h prior to measurement. Lastly, the assembled multilayer films were floated off the mica and transferred onto nylon sample holders (washers) with 10 mm diameter holes.

Both MApyrene-labeled and neat PS chains used in this study were of sufficiently high MW to ensure that interlayer diffusion occurred over at most 1−2 nm during the experimental measurement time, including the time to create a consolidated film. Estimation of interlayer diffusion of similar bilayer films has been described elsewhere.[10,16,56]

Fluorescence was measured using a Photon Technology International fluorimeter with 3−6 nm bandpass excitation and 3 nm bandpass emission slits. Film temperature was controlled by a microprocessor controller (Minco Products) with a Kapton ribbon heater attached to a flat aluminum plate that was also used as a clamping device to hold the sample. For free-standing films, the nylon washers holding the polymer films were placed and clamped between two aluminum plates that had 15 mm diameter holes in order to accommodate the excitation and emission of fluorescence from the freely standing films. A quartz cover was placed on top of the aluminum plates, and a clamping device held all the pieces together. The excitation wavelength was 324 nm, and the fluorescence emission intensity was monitored at 370−415 nm.

All fluorescence-based T_g measurements were obtained upon cooling from the rubbery or liquid state. Films that exhibited T_g > 343 K (T_g < 343 K) were initially heated to at least T_g + 40 K (383 K) and held for a minimum of 20 min before measuring the emission spectrum at elevated temperature in the rubbery state. The temperature was then decreased by 5 K at a time, and at each temperature the sample was held for 5 min to ensure thermal equilibrium before measuring the emission spectrum. In order to measure T_g, we used the temperature dependence

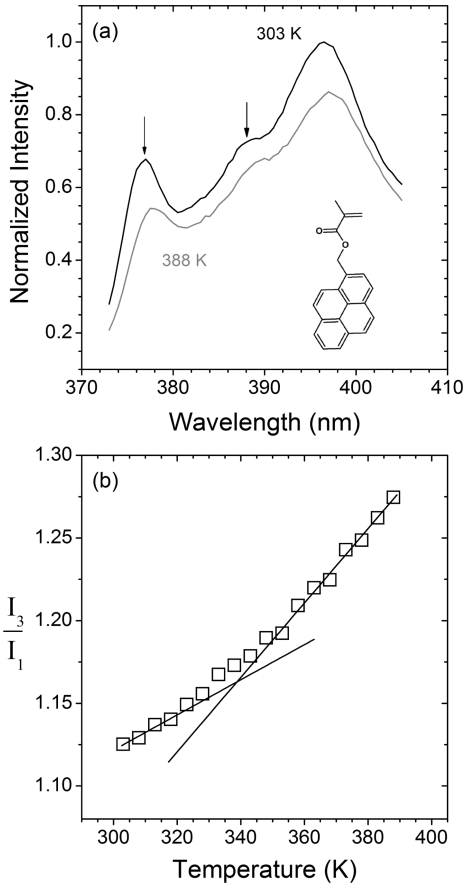

Figure 1. (a) Temperature dependence of the fluorescence emission spectrum of a 56 nm thick free-standing MApyrene-labeled PS film. (1.2 wt % of the polymer repat units contain pyrene dye.) Spectra have been normalized to one by the peak intensity in the 303 K emission spectrum. Arrows indicate the approximate wavelengths at which I_1 and I_3 intensities are measured. Inset: molecular structure of MApyrene. (b) Temperature dependence of the ratio of intensities at the third and first peaks of a 56 nm thick MApyrene-labeled PS film. (Data were obtained upon cooling.)

of the ratio of the intensity of the third peak to the intensity of the first peak (I_3/I_1) of the pyrenyl dye label emission spectrum. The intensity ratio was obtained by dividing the intensity of the third peak maximum located at 386.0 ± 3.5 nm by the intensity of the first peak maximum located at 375.0 ± 3.5 nm, and intensities were averaged over a 1−2 nm range (using data at each 0.5 nm). In fitting the temperature dependences of I_3/I_1 in the rubbery and glassy states, data points well outside T_g were used for the linear fits. To initiate the fitting procedure, data points were added to the rubbery- and glassy-state linear regressions at the extrema in the temperature range of the data. Related details on determination of T_g values from fits to temperature-dependent fluorescence data are provided in previous studies.[6,10,47−49]

RESULTS AND DISCUSSION

Figure 1a illustrates the significant effect of temperature on the spectral shape of the fluorescence of MApyrene-labeled PS in a single-layer 56 nm thick free-standing film. It is well-known that the ratio of the intensity of the third peak to the intensity of the first peak, I_3/I_1, of the pyrene emission spectrum is sensitive to polarity of the local dye environment.[50,51] (When excited-state pyrene is in a polar environment, its molecular orbitals distort,

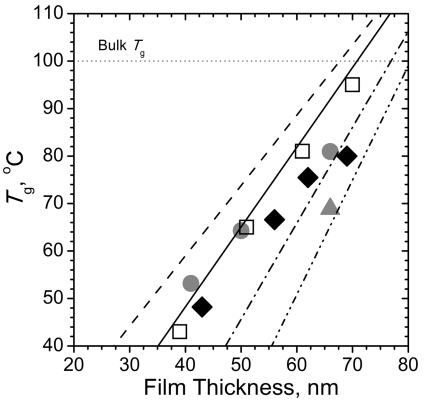

Figure 2. Thickness dependence of T_g in nanoconfined free-standing MApyrene-labeled PS films: M_n = 805 kg mol^{-1} (solid black diamonds), M_n = 701 kg mol^{-1} (solid gray circles) from ref 47, and M_n = 1460 kg mol^{-1} (solid gray triangle) from ref 47. The open square symbols are T_g values of PS free-standing films with M_n = 691 kg mol^{-1} reported by Dalnoki-Veress et al.[24,25] Diagonal lines are best fits to data reported by Dalnoki-Veress et al.:[24,25] M_n = 514 kg mol^{-1} (dashed line), M_n = 691 kg mol^{-1} (solid line), M_n = 1180 kg mol^{-1} (dash-dot line), and M_n = 2070 kg mol^{-1} (dash-dot-dot line).

resulting in an increase of the intensity of the 0−0 band (I_1) relative to other peaks,[50,51] with I_3/I_1 correlating quantitatively with solvent polarity sensed by pyrene.[50]) Moreover, we have recently demonstrated that the temperature dependence of I_3/I_1 of pyrene dyes doped into or covalently attached in specific ways to polymer yields T_g values of polymer films.[47,57] Figure 1b provides plots of I_3/I_1 as a function of temperature above and below the T_gs of the 56 nm thick MApyrene-labeled PS free-standing film. (The arrows in Figure 1a indicate the approximate wavelengths at which the intensities of the first and third fluorescence peaks are measured.) The lines in Figure 1b are fits to the rubbery-state and glassy-state temperature data well above and below T_g, the value of which is determined from the intersection of the two lines, with T_g = 340 K or 67 °C for the 56 nm thick film.

Figure 2 compares the T_gs of MApyrene-labeled PS free-standing films with M_n = 805 kg mol^{-1} (M_w = 1055 kg mol^{-1}) obtained in the present study using the self-referencing fluorescence method with data from ref 47 (also using the self-referencing fluorescence method) for PS with M_n = 701 kg mol^{-1} (M_w = 917 kg mol^{-1}) and data by Dalnoki-Veress et al.[24,25] for PS with M_n = 691 kg mol^{-1} (M_w = 767 kg mol^{-1}). The figure shows a T_g-confinement effect in free-standing PS films over the thickness range 20−80 nm. Our data for the PS sample with M_n = 805 kg mol^{-1} show the expected behavior, falling between the Dalnoki-Veress et al. fit lines[24,25] for free-standing films with M_n = 691 kg mol^{-1} and M_n = 1180 kg mol^{-1}. It is also noteworthy that the T_gs of the PS free-standing films with M_n = 805 kg mol^{-1} in the current study are generally lower than the T_gs obtained in our previous self-referencing fluorescence study of PS free-standing films with similar thicknesses but lower MW (M_n = 701 kg mol^{-1}). For example, a 43 nm thick film with M_n = 805 kg mol^{-1} exhibits a T_g of 321 K or 48 °C ($T_g - T_{g,bulk}$ = ∼ −54 K), while a 41 nm thick film with M_n = 701 kg mol^{-1} exhibits a T_g of 326 K or 53 °C ($T_g - T_{g,bulk}$ = ∼ −49 K). Overall, the data for single-layer free-standing PS films with M_n = 805 and 701 kg mol^{-1} obtained using the self-referencing fluorescence method are in reasonable agreement with (and reflect the MW dependence of) the data by Forrest, Dalnoki-Veress, and Dutcher.[24,25]

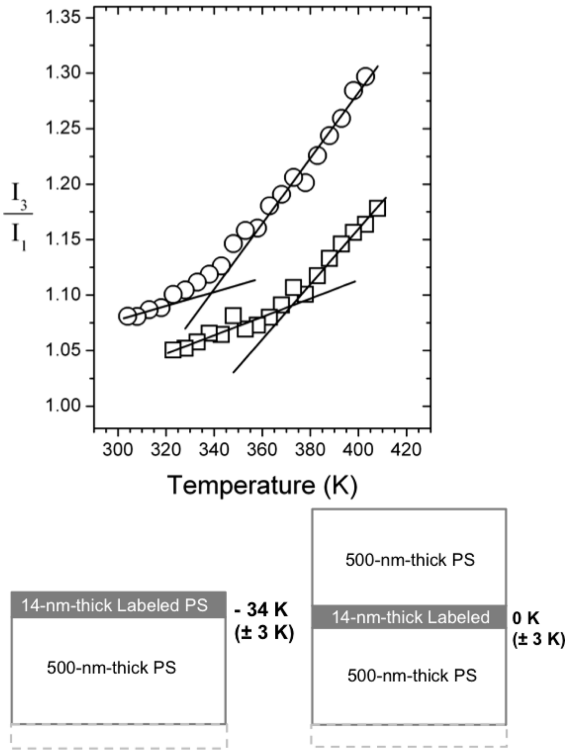

Figure 3. Temperature dependence of the ratio of intensities at the third and first peaks (I_3/I_1) of a 14 nm thick MApyrene-labeled PS free-surface layer (circles) and a 14 nm thick MApyrene-labeled PS middle layer (squares) in free-standing bulk PS films.

Figure 3 shows the temperature dependence of I_3/I_1 for a 14 nm thick MApyrene-labeled PS free-surface layer and a 14 nm thick MApyrene-labeled PS middle layer in trilayer free-standing bulk PS films. The lines in the plot are fits to the rubbery-state and glassy-state temperature data well above and below T_g, the value of which is determined from the intersection. The 14 nm thick free-surface layer sitting atop a 500 nm thick neat PS underlayer (not supported on a substrate) yields $T_g - T_{g,bulk}$ = −34 ± 3 K; the 14 nm thick middle layer sandwiched between 500 nm thick neat PS layers exhibits bulk T_g within experimental error. These local T_gs in the free-surface and middle layers are, within experimental error, identical to the T_gs reported by Ellison and Torkelson[10] within similar layers of substrate-supported bulk PS films. They showed that a 14 nm thick free-surface layer sitting atop a 270 nm thick PS substrate-supported film yields $T_g - T_{g,bulk}$ = ∼ −32 K.[10] Also, when a 14 nm thick labeled middle layer was sandwiched between two 270 nm thick neat PS layers (with the underlayer supported by a silica substrate), the middle layer exhibited the bulk T_g,[10] in accordance with our data in the trilayer bulk free-standing film. These results indicate that the cooperative segmental mobility associated with T_g very near the free surface of a bulk free-standing PS film is significantly greater than that of bulk PS and that similar behavior is observed in the free-surface layer of a bulk supported PS film.

Figure 4 summarizes our results with 56 nm thick multilayer free-standing PS films, identical in thickness to the single-layer film characterized in Figures 1 and 2. As shown in Figure 2, a 56 nm thick single-layer free-standing PS film with M_n = 805 kg mol^{-1} exhibits $T_g - T_{g,bulk}$ = ∼ −33 K. Using a 56 nm thick bilayer free-standing film, we find that the 14 nm thick

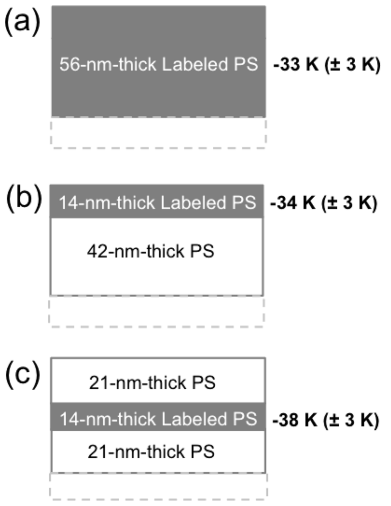

Figure 4. $T_g - T_{g,bulk}$ in free-standing labeled PS films and layers: (a) single-layer 56 nm thick film, (b) 14 nm thick free-surface layer within a bilayer film of 56 nm total thickness, (c) 14 nm thick middle-layer within a trilayer film of 56 nm total thickness. (The data for I_3/I_1 as a function of temperature for the bilayer and trilayer films, resulting in T_g determinations, are provided in the Supporting Information.)

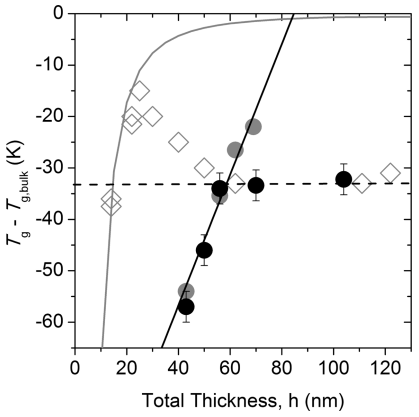

Figure 5. Comparison of free-surface layer T_gs in bilayer free-standing PS films to free-surface layer T_gs in bilayer substrate-supported PS films. The black circles represent T_g values of 14 nm thick labeled PS free-surface layers as a function of total thickness of bilayer free-standing PS films. The gray circles represent T_g values of single layer labeled PS free-standing films with M_n = 805 kg mol^{-1} from Figure 2, and the solid black line is a best fit to the single-layer T_g values. The data are compared to results from ref 10 for substrate-supported PS films. Diamonds represent T_g values identified by fluorescence intensity for 14 nm thick labeled PS free-surface layers of bilayer supported films as a function of total bilayer film thickness.[10] The solid gray curve is a fit of $T_g(h) = T_{g,bulk}[1 - (A/h)^\delta]$ to the thickness dependence data from single layer pyrene-doped PS supported films in ref 10 (A = 4.3, δ = 2.0, and $T_{g,bulk}$ = 373 K). The horizontal line represents $T_g - T_{g,bulk}$ of the 14 nm thick free-surface layer which is independent of underlayer thickness and film geometry for both free-standing and substrate-supported films.

MApyrene-labeled surface layer exhibits a T_g value ($T_g - T_{g,bulk} = -34 \pm 3$ K) that is within error identical to the average T_g of the single-layer film. This surface layer T_g is also identical within error to the T_g of a 14 nm thick free-surface layer atop a free-standing bulk PS film.

Using a 56 nm thick trilayer free-standing film, we find that the 14 nm thick labeled middle layer exhibits $T_g - T_{g,bulk} = -38 \pm 3$ K, which within error agrees with the average T_g of the 56 nm thick single-layer film but is 38 K below the T_g of a 14 nm thick middle layer in a bulk trilayer PS film. Thus, in comparison with a bulk free-standing film exhibiting a large difference between the T_gs in a 14 nm thick layer in the middle and at the free surface and thereby a gradient in T_g across the film, no T_g gradient is apparent using 14 nm thick labeled layers within a 56 nm thick free-standing PS film. We hypothesize that a much narrower distribution of T_gs is present in nanoconfined films because the average cooperative dynamics associated with the middle layer T_g are significantly impacted by the average cooperative segmental dynamics in the surface layers, at most ~20 nm away. Thus, when the thickness of a PS free-standing film is 56 nm, the T_g gradient is eliminated (as characterized by 14 nm thick layers). A related suppression of a T_g gradient was observed by Ellison and Torkelson[10] in sufficiently thin substrate-supported PS films: for bilayer films with a total thickness of 24 nm, a 12 nm thick labeled surface layer exhibited a T_g that was within error identical to the average T_g across the film ($T_{g,bulk} - 11$ K).

As shown in Figure 5, in the case of substrate-supported bilayer PS films (data from ref 10), when the total film thickness exceeds 60 nm, a 14 nm thick surface layer exhibits a T_g that is 32 K below $T_{g,bulk}$. As the total thickness decreases below 60 nm and approaches 25 nm, there is a sharp increase in the surface layer T_g. At a total thickness below ~25 nm, the surface layer exhibits a T_g value that is within error identical to the average across the film. As described in ref 10, these results for substrate-supported PS films have been understood in the following manner. At thicknesses exceeding 60 nm, the films exhibit the full gradient in T_g, from a sharply reduced local T_g near the free surface to bulk T_g within the film interior, observed in bulk PS films. When the total thickness is below ~60 nm, the dynamics adjust to satisfy the constraint that the T_g gradient from surface to substrate is not too sharp and abrupt; i.e., when the substrate-supported film is too thin, it cannot support the full gradient in glass transition dynamics observed in bulk PS films. When the total thickness is below a critical value, ~25 nm as observed via 12 or 14 nm thick labeled surface layers, the thickness is insufficient to accommodate a substantial, smooth gradient in T_g from surface to substrate.

We note that the 56 nm thick free-standing PS film in our current study, which shows no T_g gradient as determined by 14 nm thick labeled layers, is almost exactly twice the thickness for which an absence of a T_g gradient was determined by Ellison and Torkelson[10] in substrate-supported PS films (~25 nm). These results suggest that ~56 nm may be close to the critical thickness for PS free-standing films (with M_n = 805 kg mol^{-1} and possibly other MWs) at which T_g gradients are suppressed (as observed with 14 nm thick labeled layers) because of the propagation of the strongly perturbed free-surface T_g from both free surfaces across the film. This hypothesis is also supported by a recent experimental study by Napolitano and Wubbenhorst;[58] using dielectric spectroscopy, they showed that there is asymmetric broadening of the structural relaxation peak of PS free-standing films toward lower temperatures and that the broadening decreases with decreasing thickness. They suggested that because of free-surface effects from both film surfaces, free-standing PS films thinner than a threshold thickness cannot contain any bulk component, resulting in the smaller broadening of the structural relaxation peak with decreasing thickness.

Figure 5 shows details of how the underlayer thickness of free-standing bilayer PS films affects the T_g of a 14 nm thick free-surface layer and compares these results to those for supported PS films from Ellison and Torkelson.[10] When the total thickness of a PS free-standing film is ~56 nm or greater, the 14 nm thick surface layer exhibits a T_g that is ~34 K below bulk T_g. Within experimental error, this result is in agreement with the results for substrate-supported PS films showing that the T_g of a 14 nm thick free-surface layer is ~32 K below bulk T_g when the total film thickness exceeds ~60 nm. However, when the total free-standing PS film thickness decreases below ~56 nm, the 14 nm thick surface layer exhibits a T_g that decreases below $T_{g,bulk}$ − 34 K with decreasing total film thickness and is within error identical to that of the average T_g across the whole film; i.e., the film exhibits no significant T_g gradient as reported by 14 nm thick labeled layers. In particular, a 43 nm thick single-layer free-standing PS film exhibits $T_g = T_{g,bulk} - \sim 54$ K, which is within error (±2−3 K) identical to $T_g = T_{g,bulk} - \sim 57$ K exhibited by a 14 nm thick free-surface layer in a 43 nm thick bilayer free-standing PS film. This behavior is the opposite of that observed in substrate-supported films with thicknesses in the range ~25−60 nm but similar to that observed in substrate-supported films with thicknesses less than ~25 nm.

The results of the free-standing PS films reported here and the results of the substrate-supported PS films reported by Ellison and Torkelson[10] are in substantial agreement with and complement each other. When total film thickness is ~56−60 nm or greater, a 14 nm thick free-surface layer exhibits a T_g value that is ~32−34 K below $T_{g,bulk}$, regardless of whether the film is free-standing or substrate-supported. This may be understood from the standpoint that the local T_g behavior at the opposite interface (polymer−air in the case of a free-standing film and polymer−substrate in the case of a supported film) cannot propagate across a PS film of 56−60 nm thickness and thereby perturb the T_g response of the labeled free-surface layer.

With decreasing thickness below ~56−60 nm, a 14 nm thick free-surface layer exhibits a T_g that is strongly perturbed by the nanoscale confinement of the whole film, with the surface-layer T_g being impacted by the presence of the interface (polymer−air or polymer−substrate) on the opposite side of the film. In the case of free-standing PS films, the presence of a second free-surface only several tens of nanometers away from the labeled free-surface layer perturbs the T_g response of the labeled layer, resulting in net reduction in the observed T_g in the free-surface layer and averaged across the film as a whole. In contrast, with substrate-supported PS films in the thickness range ~25−60 nm, the propagation across the whole thickness of the T_g behaviors present at both interfaces not only inhibits a reduction of the free-surface layer T_g but also results in an increase in the free-surface layer T_g with decreasing thickness. With sufficiently thin supported PS films (less than ~25 nm thick), the films are unable to support a significant gradient in T_g dynamics across the film, leading to an apparent suppression of the T_g gradient. This ~25 nm thickness is roughly one-half the thickness at which the apparent full suppression of the T_g gradient is observed in free-standing PS films, which is caused by the effects of two free surfaces propagating into and across the free-standing films.

While the results for the distribution of T_gs obtained with our free-standing PS films can be understood to be consistent with the results for the distribution of T_gs reported earlier[10] for substrate-supported PS films, they also refute a basic consequence associated with de Gennes' "sliding motion" mechanism.[28,29] A key hypothesis of this mechanism is that the loops of a chain present at a free surface can transport "kinks" of free volume along the chain's own length, allowing for faster structural relaxation and thereby inducing a reduction in local T_g inside the film. As discussed by Binder,[30] de Gennes' sliding motion mechanism yielding faster structural relaxation can come into play only when the film thickness is less than the radius (or, more quantitatively, less than ~4 times the radius) of a chain in the film, thereby allowing the formation of loops at the free surface from segments of chains that extend into the middle of and possibly even across the film thickness. A consequence of this is that T_g reductions are not expected in a middle layer of a consolidated trilayer film that has been constructed, as in the current study, to disallow any chain in the middle layer from forming loops at the free surface of the trilayer film.

As mentioned earlier, both MApyrene-labeled and neat PS chains used in this study are of sufficiently high MW (M_n = 805 000 g mol^{-1} and M_w/M_n = 1.31 for MApyrene-labeled PS and M_n = 849 000 g mol^{-1} and M_w/M_n = 1.06 for neat PS) to ensure that interlayer diffusion occurs over at most 1−2 nm during the experimental measurement time, which includes the time to create a consolidated film.[10,16,56] Given this fact, in our 56 nm thick PS trilayer free-standing film, no MApyrene-labeled PS chain in a 14 nm thick middle layer can form loops or bridges in contact with the free surfaces. However, as shown in Figures 3 and 4, the 14 nm thick middle layer of the 56 nm thick PS trilayer free-standing film exhibits a T_g that within error is identical to the T_g of 14 nm thick surface layers and the overall average T_g within a single-layer 56 nm thick film.

The results of our multilayer free-standing film study can be understood by appreciating that the average cooperative segmental dynamics associated with T_g within a middle layer at a particular film depth are impacted by the strongly perturbed, average cooperative dynamics present several tens of nanometers away near the free surface, without the need for chains within the middle layer to have segments forming loops at polymer−air interfaces. This also explains why the onset thickness for and the size of the T_g reduction relative to $T_{g,bulk}$ with decreasing thickness are larger in free-standing than in substrate-supported PS films. Our current study and previous work[47] provide support for the MW dependence of the T_g-confinement effect in free-standing PS films reported by Dutcher and co-workers,[22−25] which is not observed in substrate-supported PS films.[48] Our current study and previous work[10,47,48] on free-standing and substrate-supported films applied thermal histories prior to and during measurement that were similar to each other but different from those used by Dutcher and co-workers[22−25] in their free-standing film studies. This indicates that experimental artifacts such as the specific annealing conditions used by Dutcher and co-workers are not the origin of the strong effect of MW on the T_g-confinement behavior observed in free-standing PS films. Finally, outside of refuting the "sliding motion" model by de Gennes,[21] our current study does not yield an understanding of this effect or suggest an origin for this effect.

We note that Lipson and Milner[40,41] recently considered the effects of MW on the T_g-confinement effect in free-standing and semi-infinite PS films. Following de Gennes' "sliding mechanism",[28,29] they developed a delayed glassification theory to predict quantitatively the effects of MW and film thickness on T_g for both semi-infinite (related to substrate-supported) and free-standing film geometries. They constructed a quantitative description of the influences of the free surface and polymer MW on average T_g via transmission of "kinks" or "free volume" along

the chain backbone from loops starting or ending at the free surface. In semi-infinite and free-standing PS films, their approach yields dramatic reductions in average T_g relative to the bulk value with decreasing film thickness, as observed in many experimental studies. While their calculations yielded a significant MW dependence of average T_g in free-standing films, qualitatively in accord with experiment, the MW dependence disappeared in the thinnest films, the opposite of what is observed in the experimental studies by Dutcher and co-workers.[22−25] This result may be taken as further evidence against the "sliding mechanism". Their calculations also yielded interesting results in semi-infinite films, with a prediction of a MW dependence of the T_g reported from a labeled top layer (with variable thickness h) in a semi-infinite bilayer film. Lipson and Milner[41] stated that their model predictions for this case had not yet been experimentally tested, suggesting that studies were needed to determine whether a MW effect is evident in the h-dependence of the free-surface layer T_g in semi-infinite films.

A comparison of the results of our present study with those of Ellison and Torkelson[10] reveals the same T_g reduction within error ($T_g = T_{g,bulk} - \sim 32-34$ K) in 14 nm thick free-surface layers sitting atop free-standing and substrate-supported PS films with overall thickness greater than or equal to ∼56−60 nm. (In such film geometries, the substrate-supported film corresponds to a semi-infinite film when the film thickness is sufficiently large to suppress any effect of the substrate on the response of the free-surface layer.) However, the PS samples used in the current study and by Ellison and Torkelson[10] differ by nearly a factor of 2 in M_n values, 805 kg mol^{-1} vs 440 kg mol^{-1}, and have MWs exactly in the range where Lipson and Milner[41] predicted the largest effect of MW on the PS free-surface layer T_g. Clearly, this limited experimental comparison does not provide a comprehensive test of the predictions of the Lipson−Milner model, which in turn is related to (i.e., develops the detailed consequences of the basic idea of) de Gennes' sliding motion mechanism. However, our results do not suggest that a significant MW dependence, which is absent in the T_g-confinement effect in single-layer supported PS films, will be experimentally observed in nanoconfined free-surface layers atop semi-infinite PS films.

Further studies of the type undertaken in the present study and by Ellison and Torkelson[10] may provide a fully comprehensive test of the predictions of the model by Lipson and Milner.[41] Additional self-referencing fluorescence studies of free-standing films of polymers other than PS are also warranted, as are investigations of effects of confinement on polymer properties other than T_g. Finally, further experimental and theoretical investigations will be needed to unravel the puzzle that remains associated with the different roles of MW in the T_g-confinement effects in free-standing and supported PS films.

■ ASSOCIATED CONTENT

Ⓢ Supporting Information. Figure S1 reports data for I_3/I_1 as a function of temperature for the bilayer and trilayer films in Figure 4, resulting in T_g determinations. This material is available free of charge via the Internet at http://pubs.acs.org.

■ AUTHOR INFORMATION

Corresponding Author

*E-mail: j-torkelson@northwestern.edu.

■ ACKNOWLEDGMENT

We acknowledge the support of the NSF-MRSEC Program (Grant DMR-0520513), Northwestern University, and a Terminal-Year Fellowship (to S.K).

■ REFERENCES

(1) Keddie, J. L.; Jones, R. A. L.; Cory, R. A. *Europhys. Lett.* **1994**, *27*, 59–64.
(2) Keddie, J. L.; Jones, R. A. L.; Cory, R. A. *Faraday Discuss.* **1994**, *98*, 219–230.
(3) Forrest, J. A.; Dalnoki-Veress, K. *Adv. Colloid Interface Sci.* **2001**, *94*, 167–196.
(4) Alcoutlabi, M.; McKenna, G. B. *J. Phys.: Condens. Matter* **2005**, *17*, R461–R524.
(5) Roth, C. B.; Dutcher, J. R. *J. Electroanal. Chem.* **2005**, *584*, 13–22.
(6) Kim, S.; Hewlett, S. A.; Roth, C. B.; Torkelson, J. M. *Eur. Phys. J. E* **2009**, *30*, 83–92.
(7) Reiter, G.; Napolitano, S. *J. Polym. Sci., Part B: Polym. Phys.* **2010**, *48*, 2544–2547.
(8) Hall, D. B.; Underhill, P.; Torkelson, J. M. *Polym. Eng. Sci.* **1998**, *38*, 2039–2045.
(9) In contrast to the dozens of studies cited in refs 3−7 noting a significant dependence of T_g on thickness in nanoconfined PS films as measured by a wide array of experimental techniques and researchers, we note that there are a small number of reports indicating the absence of such a dependence. See, for example, the following: Tress, M.; Erber, M.; Mapesa, E. U.; Huth, H.; Muller, J.; Serghei, A.; Schick, C.; Eichhorn, K. J.; Volt, B.; Kremer, F. *Macromolecules* **2010**, *43*, 9937–9944.
(10) Ellison, C. J.; Torkelson, J. M. *Nature Mater.* **2003**, *2*, 695–700.
(11) Ellison, C. J.; Torkelson, J. M. *J. Polym. Sci., Part B: Polym. Phys.* **2002**, *40*, 2745–2758.
(12) Priestley, R. D.; Broadbelt, L. J.; Torkelson, J. M. *Macromolecules* **2005**, *38*, 654–657.
(13) Priestley, R. D.; Ellison, C. J.; Broadbelt, L. J.; Torkelson, J. M. *Science* **2005**, *309*, 456–459.
(14) Roth, C. B.; McNerny, K. L.; Jager, W. F.; Torkelson, J. M. *Macromolecules* **2007**, *40*, 2568–2574.
(15) Roth, C. B.; Torkelson, J. M. *Macromolecules* **2007**, *40*, 3328–3336.
(16) Priestley, R. D.; Mundra, M. K.; Barnett, N.; Broadbelt, L. J.; Torkelson, J. M. *Aust. J. Chem.* **2007**, *60*, 765–771.
(17) Inoue, R.; Kawashima, K.; Matsui, K.; Kanaya, T.; Nishida, K.; Matsuba, G.; Hino, M. *Phys. Rev. E* **2011**, *83*, 021801.
(18) (a) Priestley, R. D.; Broadbelt, L. J.; Torkelson, J. M.; Fukao, K. *Phys. Rev. E* **2007**, *75*, 061806.(b) Priestley, R. D. Ph.D. Thesis, Northwestern University, 2008.
(19) Peter, S.; Napolitano, S.; Meyer, H.; Wubbenhorst, M.; Baschnagel, J. *Macromolecules* **2008**, *41*, 7729–7743.
(20) Fakhraai, Z.; Forrest, J. A. *Science* **2008**, *319*, 600–604.
(21) Yang, Z. H.; Fujii, Y.; Lee, F. K.; Lam, C. H.; Tsui., O. K. C. *Science* **2010**, *328*, 1676–1679.
(22) Forrest, J. A.; Dalnoki-Veress, K.; Dutcher, J. R. *Phys. Rev. E* **1997**, *56*, 5705–5716.
(23) Forrest, J. A.; Dalnoki-Veress, K.; Stevens, J. R.; Dutcher, J. R. *Phys. Rev. Lett.* **1996**, *77*, 2002–2005.
(24) Dalnoki-Veress, K.; Forrest, J. A.; de Gennes, P. G.; Dutcher, J. R. *J. Phys. IV* **2000**, *10*, 221–226.
(25) Dalnoki-Veress, K.; Forrest, J. A.; Murray, C.; Gigault, C.; Dutcher, J. R. *Phys. Rev. E* **2001**, *63*, 031801.
(26) Roth, C. B.; Dutcher, J. R. *Eur. Phys. J. E* **2003**, *12*, S103–S107.
(27) Roth, C. B.; Pound, A.; Kamp, S. W.; Murray, C. A.; Dutcher, J. R. *Eur. Phys. J. E* **2006**, *20*, 441–448.
(28) de Gennes, P. G. *C. R. Acad. Sci., Ser. IV: Phys., Astrophys.* **2000**, *1*, 1179–1186.
(29) de Gennes, P. G. *Eur. Phys. J. E* **2000**, *2*, 201–203.
(30) Binder, K. *Eur. Phys. J. E* **2000**, *2*, 204.

(31) Mattsson, J.; Forrest, J. A.; Borjesson, L. *Phys. Rev. E* **2000**, *62*, 5187–5200.
(32) Liem, H.; Cabanillas-Gonzalez, J.; Etchegoin, P.; Bradley, D. D. C. *J. Phys.: Condens. Matter.* **2004**, *16*, 721–728.
(33) Miyazaki, T.; Inoue, R.; Nishida, K.; Kanaya, T. *Eur. Phys. J. Spec. Top.* **2007**, *141*, 203–206.
(34) Svanberg, C. *Macromolecules* **2007**, *40*, 312–315.
(35) O'Connell, P. A.; Hutcheson, S. A.; McKenna, G. B. *J. Polym. Sci., Part B: Polym. Phys.* **2008**, *46*, 1952–1965.
(36) O'Connell, P. A.; McKenna, G. B. *Eur. Phys. J. E* **2006**, *20*, 143–150.
(37) O'Connell, P. A.; McKenna, G. B. *Science* **2005**, *307*, 1760–1763.
(38) Jain, T. S.; de Pablo, J. J. *Phys. Rev. Lett.* **2004**, *92*, 155505.
(39) Rotella, C.; Napolitano, S.; Wubbenhorst, M. *Macromolecules* **2009**, *42*, 1415–1417.
(40) Lipson, J. E. G.; Milner, S. T. *Macromolecules* **2010**, *43*, 9874–9880.
(41) Milner, S. T.; Lipson, J. E. G. *Macromolecules* **2010**, *43*, 9865–9873.
(42) Peter, S.; Meyer, H.; Baschnagel, J. *J. Phys.: Condens. Matter* **2007**, *19*, 205119.
(43) Jones, R. A. L. *Eur. Phys. J. E* **2000**, *2*, 205.
(44) Baljon, A. R. C.; Williams, S.; Balabaev, N. K.; Paans, F.; Hudzinskyy, D.; Lyulin, A. V. *J. Polym. Sci., Part B: Polym. Phys.* **2010**, *48*, 1160–1167.
(45) Lipson, J. E. G.; Milner, S. T. *Eur. Phys. J. B* **2009**, *72*, 133–137.
(46) Stevenson, J. D.; Wolynes, P. G. *J. Chem. Phys.* **2008**, *129*, 324514.
(47) Kim, S.; Roth, C. B.; Torkelson, J. M. *J. Polym. Sci., Part B: Polym. Phys.* **2008**, *46*, 2754–2764.
(48) Ellison, C. J.; Mundra, M. K.; Torkelson, J. M. *Macromolecules* **2005**, *38*, 1767–1778.
(49) Rittigstein, P.; Torkelson, J. M. *J. Polym. Sci., Part B: Polym. Phys.* **2006**, *44*, 2935–2943.
(50) Kalyanasundaram, K.; Thomas, J. K. *J. Am. Chem. Soc.* **1977**, *99*, 2039–2044.
(51) Nakashima, K.; Winnik, M. A.; Dai, K. H.; Kramer, E. J.; Washiyama, J. *Macromolecules* **1992**, *25*, 6866–6870.
(52) Kim, S. D.; Torkelson, J. M. *Macromolecules* **2002**, *35*, 5943–5952.
(53) Duhamel, J. In *Molecular Interfacial Phenomena of Polymers and Biopolymers*; Chen, P., Ed.; Woodhead Publishing: Cambridge, England, 2005; pp 214−248.
(54) Colambani, O.; Ruppel, M.; Schubert, F.; Zettl, H.; Pergushov, D. V.; Muller, A. H. E. *Macromolecules* **2007**, *40*, 4338–4350.
(55) Roth, C. B.; Pound, A.; Kamp, S. W.; Murray, C. A.; Dutcher, J. R. *Eur. Phys. J. E* **2006**, *20*, 441–448.
(56) Whitlow, S. J.; Wool, R. P. *Macromolecules* **1991**, *24*, 5926–5938.
(57) As described in ref 53, free pyrene dye and pyrene covalently attached to a polymer via a methylene linking group exhibit I_3/I_1 values that are strongly sensitive to polarity; however, a longer linking group leads to a loss of sensitivity to polarity. We demonstrated in ref 47 that the temperature dependence of I_3/I_1 yields a clear determination of the T_g of supported and free-standing polymer films when the pyrene dye is attached to the polymer via a methylene linking unit, as in the case of 1-pyrenylmethyl methacrylate-labeled PS (MApyrene-labeled PS). However, when a butylene linking unit is used, as with 1-pyrenylbutyl methacrylate-labeled PS (BApyrene-labeled PS in ref 47), T_g cannot be determined via the temperature dependence of I_3/I_1 of supported or free-standing polymer films, although the temperature dependence of the integrated fluorescence intensity (across the whole emission spectrum) yields T_g in supported polymer films.
(58) Napolitano, S.; Wubbenhorst, M. *Polymer* **2010**, *51*, 5309–5312.